

QUASISYMMETRIC EMBEDDING OF SELF SIMILAR SURFACES AND ORIGAMI WITH RATIONAL MAPS

Daniel Meyer

University of Washington, Department of Mathematics
Box 354350, Seattle, WA 98195-4350, U.S.A.; meyer@math.washington.edu

Abstract. We show how self similar surfaces can be quasimetrically embedded in the plane. To do this we construct a rational map which realizes the self similarity. Several examples of rational maps which realize subdivision rules are presented. We also show how the Xmas tree, an embedded surface in \mathbf{R}^3 whose Hausdorff dimension can be arbitrarily close to 3, can be embedded quasimetrically in the plane.

1. Introduction

It is well known that the *snowflake* (or von Koch curve) can be mapped to a circle by a quasiconformal map of the plane. The higher dimensional analogue is to embed the *snowball* (see next section for the definition), or other self similar surfaces quasimetrically in the plane. From recent work of Cannon et al. ([CFP, Section 6]) it follows that such an embedding exists, by the use of Cannon's combinatorial Riemann mapping theorem [C]. M. Bonk and B. Kleiner in [BK] used circle packings to give another proof that such an embedding exists. We present an alternative method, which is much less general than the above methods, but has the advantages of being elementary and constructive. The main idea is to build a rational map which realizes the self similarity. This map has the nice property that every critical value is a repelling fixed point. Standard modulus estimates then show that this map induces a quasimetric embedding.

Notation. $\widehat{\mathbf{C}} = \mathbf{C} \cup \{\infty\}$ is the Riemann sphere, $\widehat{\mathbf{R}} = \mathbf{R} \cup \{\infty\} \subset \widehat{\mathbf{C}}$ the extended real line, \mathbf{H}^+ the upper half plane, \mathbf{H}^- the lower half plane. For two nonnegative expressions f, g we write $f \asymp g$ if there is a constant $C > 1$, such that $1/Cg \leq f \leq Cg$. By S^o we denote the interior of a set S .

Acknowledgments. The idea to realize a subdivision rule by a rational map is due to Rick Kenyon, see also [CFKP]. I also thank my advisor Steffen Rohde for his patience and many helpful suggestions. He also suggested the Xmas tree example in Section 6.4.

2. Definitions

2.1. Quasisymmetry. The classical paper on quasisymmetry is [TV]. We follow [H], where a detailed treatment can be found. Recall that a map is called an *embedding* if it is a homeomorphism onto its image. An embedding $f: X \rightarrow Y$ of metric spaces is called *quasisymmetric* (or η -quasisymmetric) if there is a homeomorphism $\eta: [0, \infty) \rightarrow [0, \infty)$, such that

$$(2.1) \quad |x - a| \leq t|x - b| \quad \Rightarrow \quad |f(x) - f(a)| \leq \eta(t)|f(x) - f(b)|$$

for all $x, a, b \in X$, $t \geq 0$. Quasisymmetry may be viewed as a natural generalization of quasiconformality: a homeomorphism $\mathbf{R}^n \rightarrow \mathbf{R}^n$ is quasisymmetric if and only if it is quasiconformal. However, a Möbius transformation from the unit disc to the upper half plane will not be quasisymmetric. This is easy to see, since a quasisymmetry maps bounded sets to bounded sets.

To check whether a map is quasisymmetric can be quite tedious. Therefore one often considers a weaker condition. An embedding $f: X \rightarrow Y$ of metric spaces is called *weakly quasisymmetric* (or H -weakly quasisymmetric) if there is a number $H \geq 0$, such that

$$(2.2) \quad |x - a| \leq |x - b| \quad \Rightarrow \quad |f(x) - f(a)| \leq H|f(x) - f(b)|$$

for all $x, a, b \in X$. Quasisymmetric maps are “more nicely” behaved than weakly quasisymmetric ones. Equation (2.1) implies that f is continuous and either constant or injective. If f is not constant then (2.2) implies that f^{-1} is $\tilde{\eta}$ -quasisymmetric where $\tilde{\eta}(t) = 1/\eta^{-1}(t^{-1})$ on $f(X)$. So if f is not constant (2.1) implies that f is a homeomorphism onto its image. Moreover if $f_1: X \rightarrow Y$ is η_1 -quasisymmetric and $f_2: Y \rightarrow Z$ is η_2 -quasisymmetric $f_2 \circ f_1$ is $\eta_2 \circ \eta_1$ -quasisymmetric.

On the other hand (2.2) does not imply continuity, and weak quasiconformality is in general not preserved under inverses and compositions. However in many cases quasisymmetry is implied by weak quasisymmetry, which is much easier to check. A metric space is called *doubling* if there is a number N such that every ball of diameter d can be covered by N sets of diameter at most $\frac{1}{2}d$, for all $d > 0$.

Theorem 2.1 ([H, Theorem 10.19]). *A weakly quasisymmetric embedding of a connected doubling space into a doubling space is quasisymmetric.*

2.2. The snowball. The snowball is a topologically 2-dimensional analogue of the snowflake (or von Koch curve). It is constructed in the following way. Divide each face of the unit cube in \mathbf{R}^n into 9 squares of sidelength $\frac{1}{3}$. Place a cube of sidelength $\frac{1}{3}$ on the middle square of each side, resulting in a body which is bounded by $6 \cdot 13$ squares of sidelength $\frac{1}{3}$. One ‘face’ consisting of 13 squares is called the *generator* of the snowball, see Figure 1.

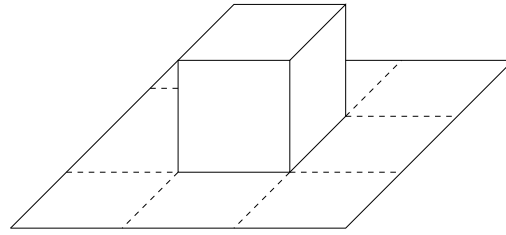


Figure 1. Generator of S .

Each of the $6 \cdot 13$ squares is then again subdivided into 9 squares of sidelength $\frac{1}{9}$, on the middle square put a cube of sidelength $\frac{1}{9}$, and so on. Let K be the limiting body. The snowball is the set of prime ends of K^o . Let S be the part of the snowball that corresponds to one side of the original cube. In each step the 13^n squares get replaced by scaled copies of the generator. Let S_n be the surface after n steps, S_0 being the unit square. The boundary ∂K of K has self-intersections, see Figure 2. This is the reason why we take prime ends. In S the two points indicated by the arrows are distinct.

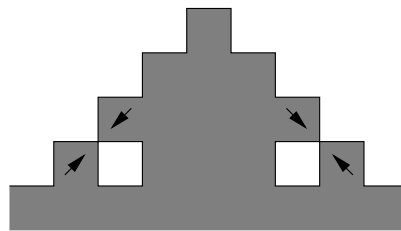


Figure 2. Cut through S_2 .

S is naturally divided into 13 pieces which correspond to the 13 squares that make up S_1 . Each of these is naturally mapped to S by stretching, rotating, and translating. The rational map constructed in the next section will represent this selfsimilarity.

In the same way as above S consists of 13^n copies of itself, scaled by a factor of 3^{-n} . These are called *cylinders* of order (or length) n , or n -cylinders. For such a cylinder X the notation $|X| = n$ is used. For each point $x \in S$ there is a sequence of cylinders such that

$$(2.3) \quad S = X_0 \supset X_1 \supset X_2 \cdots, \quad \bigcap_n X_n = \{x\}, \quad |X_n| = n.$$

In general this sequence is not unique.

An alternative definition that avoids prime ends may be given as follows. We have two representations of the generator (and hence of S): in \mathbf{R}^3 as in Figure 1, and in \mathbf{R}^2 as in Figure 3. We use the representation in \mathbf{R}^2 to define the *topology* on S . The representation in \mathbf{R}^3 will be used to define the *metric* on S in the next section.

where n is the smallest number such that there exist cylinders $X \ni x, Y \ni y, |X| = |Y| = n$, such that

$$X \cap Y = \emptyset.$$

A slight variation of $\tilde{\delta}$ will later be denoted by δ . Note that $\tilde{\delta}$ is not a metric since it does not satisfy the triangle inequality, as one can see in Figure 4. Here we have $\tilde{\delta}(x, y) = \frac{1}{3} > \tilde{\delta}(x, z) + \tilde{\delta}(z, y) = \frac{1}{9} + \frac{1}{9}$. For our purposes however it is as good as the internal metric.

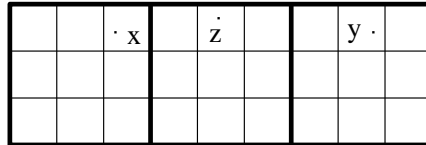


Figure 4.

Lemma 2.2. We have $\tilde{\delta}(x, y) \leq d_{\text{int}}(x, y) \leq 12 \cdot \tilde{\delta}(x, y)$, for all $x, y \in S$.

Proof. Let $\tilde{\delta}(x, y) = 3^{-n}$. The first inequality is easily seen. Let $X_n \ni x, Y_n \ni y, |X_n| = |Y_n| = n, X_n \cap Y_n = \emptyset$. Then each path from x to y must pass through the ring of cylinders of order n which have nonempty intersection with X_n . Each such path has length at least 3^{-n} .

For the second inequality let $X_{n-1} \ni x, Y_{n-1} \ni y$ be cylinders of order $n-1$. By definition of $\tilde{\delta}$ we know that X_{n-1} and Y_{n-1} intersect at least in a common corner z . By the argument in the last section

$$d_{\text{int}}(x, y) \leq d_{\text{int}}(x, z) + d_{\text{int}}(z, y) \leq 2 \cdot 3^{-n+1} + 2 \cdot 3^{-n+1} = 12\tilde{\delta}(x, y). \quad \square$$

3. Representing the snowball by a rational map

Cut S along the diagonals into 4 pieces. From now on we will only look at one such piece T . Since this contains a small copy of S it is enough to embed T quasymmetrically. Also each cylinder gets split into 4 pieces along its diagonals. From now on “cylinder” will refer to these small copies of T , and δ will denote the combinatorial pseudometric with respect to these cylinders. We have

$$(3.1) \quad \tilde{\delta}(x, y) \leq \delta(x, y) \leq 3\tilde{\delta}(x, y), \quad \text{for all } x, y \in T$$

as one easily checks. Again T consists of 13 cylinders of order 1, denoted by $T_j, 1 \leq j \leq 13$. Since the T_j ’s are scaled copies of T , there are maps

$$\tau_j: T_j \rightarrow T.$$

This gives us the standard identification of cylinders with *words*. More precisely for each cylinder X of order n we set

$$(3.2) \quad \begin{aligned} (x_0 \cdots x_{n-1}) &:= X \text{ where } x_0 = j \text{ if and only if } X \subset T_j \\ \text{and } x_k &= j \text{ if and only if } \tau_{x_{k-1}} \circ \tau_{x_{k-2}} \circ \cdots \circ \tau_{x_0}(X) \subset T_j \\ &\text{for } 1 \leq k \leq n-1. \end{aligned}$$

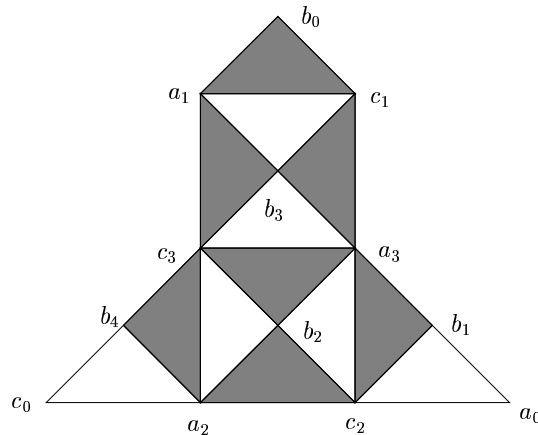


Figure 5. Generator G of T .

Note that $(x_0 \cdots x_{n+k}) \subset (y_0 \cdots y_n)$ if and only if $x_j = y_j$, $0 \leq j \leq n$.

The generator G of T is just a quarter of the generator of S . We can unfold G to map it in the plane, see Figure 5, the triangles in Figure 5 correspond to cylinders of order one. The corners of the generator G are labeled a_0 , b_0 , and c_0 , the corners of the other triangles are labeled a_k , b_l , and c_m according to Figure 5.

Now G (or more precisely the simply connected domain from Figure 5) gets mapped to the upper half plane \mathbf{H}^+ by a Riemann map, which is normalized by mapping the corners a_0 , b_0 , and c_0 to $1 =: a'_0$, $\infty =: b'_0$, and $-1 =: c'_0$ respectively (it is the inverse of a Schwarz–Christoffel map). The images of each triangle corresponding to T_j will be denoted by H_j , the images of the corners a_k , b_l , and c_m by a'_k , b'_l , and c'_m . We consider H_j to be “black” or “white” depending on whether the corresponding triangle in Figure 5 is drawn like that. By symmetry we have $a'_k = -c'_k$, $b'_1 = -b'_4$, and $b'_2, b'_3 \in i\mathbf{R}$.

Now the map R is defined in the following way:

- R on white triangles H_j is a Riemann map to the upper half plane \mathbf{H}^+ , normalized by $a'_k \mapsto 1$, $b'_l \mapsto \infty$, $c'_m \mapsto -1$;
- R on black triangles H_j is a Riemann map to the lower half plane \mathbf{H}^- with the same normalization.

Now consider two pieces H_i and H_j which share a side. H_i and H_j are reflections along this common side, since they are conformal images of real triangles for which this is true. So by reflection principle $R|_{H_i}$ extends analytically to $H_i \cup H_j$. One immediately checks that this agrees on H_j with the way it was defined before (being a Riemann map with the right normalization).

Using reflection principle again one can extend R to the whole sphere by $R(z) = \overline{R(\bar{z})}$. Another way to look at this would be to have a second copy of the generator, map it to \mathbf{H}^- , and map each of the image triangles to \mathbf{H}^+ and \mathbf{H}^- with the right normalizations.

From the construction it follows that b'_1, b'_2, b'_3, b'_4 , and $-b'_2, -b'_3$ are the poles of R . The critical points are a'_1, a'_2, a'_3 , and b'_1, b'_2, b'_3 . We can read off the order

of the poles and critical points. So R can be written in two forms:

$$(3.3) \quad R(z) = \lambda \frac{(z - 1)(z - a'_1)^3(z - a'_2)^4(z - a'_3)^5}{(z^2 - b'_1{}^2)^2(z^2 - b'_2{}^2)^2(z^2 - b'_3{}^2)^2} + 1$$

$$(3.4) \quad = \mu \frac{(z + 1)(z - c'_1)^3(z - c'_2)^4(z - c'_3)^5}{(z^2 - b'_1{}^2)^2(z^2 - b'_2{}^2)^2(z^2 - b'_3{}^2)^2} - 1,$$

where we took $b'_1 = -b'_4$ into account. By equating (3.3) and (3.4), multiplying by the denominator, and comparing coefficients, one gets a system of equations for the numbers a'_j and b'_j (using the relations $a'_j = -c'_j$). A different way to get these equations is to observe that R is an odd function.

Since the numbers a'_j and b'_j are images of the points a_j and b_j , we can obtain them from a numerical approximation of the function $G \rightarrow \mathbf{H}^+$. We used Don Marshall's program zipper

(<http://www.math.washington.edu/~marshall/zipper.html>)

for this. By using a standard Newton method for the system of equations we can increase the precision arbitrarily. We use the results from zipper as initial values, since the Newton method fails to converge otherwise.

We find that

$$\begin{aligned} a'_1 &= -69.2485\dots, \\ a'_2 &= -0.726663\dots, \\ a'_3 &= 3.33137\dots, \\ b'_1 &= 1.07729\dots, \\ b'_2 &= i \cdot 1.04067\dots, \\ b'_3 &= i \cdot 18.7881\dots, \\ \lambda &= -0.00518147\dots \end{aligned}$$

The critical values of R are -1 , 1 , and ∞ . These are repelling fixed points, so R is postcritically finite.

4. Embedding the snowball

Remark. All metrical properties such as $|x - y|$, dist and diam that occur here refer to the spherical metric, $|dz|$ denotes the length element on the sphere.

The function R induces a subdivision of the sphere into cylinders in a natural way, the cylinders of order n being the preimages of $\overline{\mathbf{H}}^+$ and $\overline{\mathbf{H}}^-$ under R^n . Each cylinder $X \subset \overline{\mathbf{H}}^+$ of order n can again be identified with the word

$$(4.1) \quad (x_0 \cdots x_{n-1}) := X, \quad x_k = j \text{ if } R^k(X) \subset H_j$$

$$(4.2) \quad \text{or } R^k(X) \subset -H_j = \{-z : z \in H_j\}.$$

Again we have $(x_0 \cdots x_{n+k}) \subset (y_0 \cdots y_n)$ if and only if $x_j = y_j$, $0 \leq j \leq n$. The n -cylinders in T form a simplicial complex, where faces, edges, and vertices (or

n -faces, n -edges, and n -vertices) are defined in the obvious way. By the combinatorics of the cylinders of n th order we mean this simplicial complex together with the inclusion relations of n -faces, n -edges, and n -vertices in k -faces, k -edges, and k -vertices, for all $k < n$. Note that the combinatorics for any n are completely determined by the combinatorics of the cylinders of first order.

Since cylinders of first order in $\overline{\mathbf{H}}^+$ are a homeomorphic image of cylinders of first order in T , their combinatorics are the same. Hence the combinatorics of any order for cylinders in T and in $\overline{\mathbf{H}}^+$ are the same.

Using (4.1) and (3.2) one gets a map

$$(4.3) \quad \text{cylinders in } T \rightarrow \text{cylinders in } \overline{\mathbf{H}}^+.$$

Lemma 4.1. *The map (4.3) induces a surjective map*

$$f: T \rightarrow \overline{\mathbf{H}}^+.$$

Proof. Since R is postcritically finite it is *subhyperbolic* (see [Mil, p. 194] and [CG, p. 91]), which means there is a metric $d_\sigma(x, y) = \inf \int_\gamma \sigma(z) |dz|$, the infimum is taken over all curves γ which connect x and y with the following properties:

- d_σ is *expanding* with respect to R , meaning there is an $A > 1$, such that

$$(4.4) \quad \sigma(R(z)) |dR(z)| \geq A\sigma(z) |dz|,$$

for all $z \in \widehat{\mathbf{C}}$;

- d_σ is *Hölder comparable* to $|x - y|$, more precisely there are constants $C > 1$, $\alpha \in (0, 1)$, such that

$$(4.5) \quad \frac{1}{C}|x - y| \leq d_\sigma(x, y) \leq C|x - y|^\alpha,$$

for all $x, y \in \widehat{\mathbf{C}}$.

Now for each $x \in T$ there is a sequence $(X_n)_{n \in \mathbf{N}}$, $|X_n| = n$ of cylinders in T such that

$$X_0 \supset X_1 \supset \dots, \quad \text{and} \quad \bigcap X_n = \{x\},$$

which gives us a mapped sequence $(X'_n)_{n \in \mathbf{N}}$ with $|X'_n| = n$, of cylinders in $\overline{\mathbf{H}}^+$ with

$$X'_0 \supset X'_1 \supset \dots.$$

By (4.4) and (4.5) we have $\text{diam } X'_n \rightarrow 0$, for $n \rightarrow \infty$. Since the X'_n are also compact we get $\bigcap X'_n = \{x'\}$, so we define

$$f(x) = x'.$$

We have to show that f is well-defined. Let $(Y_n)_{n \in \mathbf{N}}$ be a second sequence of cylinders in T , such that $|Y_n| = n$ and

$$Y_0 \supset Y_1 \supset \dots, \quad \text{and} \quad \bigcap Y_n = \{x\}.$$

Let n_0 be the smallest number, such that $X_{n_0} \neq Y_{n_0}$. From this it follows that $X_n \neq Y_n$, for all $n \geq n_0$. Since the interiors of distinct cylinders of the same order are disjoint, we get $X_n \cap Y_n = \partial X_n \cap \partial Y_n$ and $\partial X_n \cap \partial Y_n \supset \partial X_{n+1} \cap \partial Y_{n+1}$, for all $n \geq n_0$. So

$$\partial X_{n_0} \cap \partial Y_{n_0} \supset \partial X_{n_0+1} \cap \partial Y_{n_0+1} \supset \dots.$$

Since the combinatorics of the cylinders in $\overline{\mathbf{H}}^+$ are the same, we get

$$\partial X'_{n_0} \cap \partial Y'_{n_0} \supset \partial X'_{n_0+1} \cap \partial Y'_{n_0+1} \supset \dots,$$

where each $\partial X'_{n_0+j} \cap \partial Y'_{n_0+j} \neq \emptyset$ and compact. Thus $\bigcap (X'_n \cap Y'_n) \neq \emptyset$. So $\bigcap X'_n = \bigcap Y'_n = \{x'\}$, and f is well defined.

On the other hand we can find for each $x' \in \overline{\mathbf{H}}^+$ a sequence of cylinders $(X'_n)_{n \in \mathbf{N}}$ in $\overline{\mathbf{H}}^+$ as above. From this we get a sequence of cylinders $(X_n)_{n \in \mathbf{N}}$ in T , which gives an x such that $f(x) = x'$. This shows that f is surjective. \square

We now come to our main result.

Theorem 4.2. *The map*

$$f: T \rightarrow \overline{\mathbf{H}}^+$$

is a quasisymmetric embedding.

Before proving the theorem let us record some facts.

Each n -cylinder X in $\widehat{\mathbf{C}}$ gets mapped to $\overline{\mathbf{H}}^+$ or $\overline{\mathbf{H}}^-$ by R^n . We say that X is of *type* $\overline{\mathbf{H}}^+$ in the first case, of *type* $\overline{\mathbf{H}}^-$ in the second.

The preimages of the critical values -1 , 1 , and ∞ under R^n are called *corners* (or n -corners). We say an n -corner c is of *type* $R^n(c)$ ($= -1, 1$, or ∞).

The preimages of $(-\infty, -1)$, $(-1, 1)$, and $(1, \infty)$ under R^n are called *sides* or n -sides. An n -side s is of *type* $R^n(s)$ ($= (-\infty, -1), (-1, 1)$, or $(1, \infty)$).

R maps n -(cylinders, sides, corners) to $n-1$ -(cylinders, sides, corners). Since the critical values are repelling fixed points we have

$$(4.6) \quad \deg_{R^n}(z) \leq \max_{w \in \widehat{\mathbf{C}}} \deg_R(w) = 5,$$

for any $z \in \widehat{\mathbf{C}}$ and $n \geq 0$. At each n -corner c , $2 \deg_{R^n}(c)$ n -cylinders and n -sides intersect.

Two cylinders of the same order are called *neighbors* if they share a side. Neighbors always get mapped to different half planes (i.e. are of different type).

For two neighbors X, Y of order n with shared side s the map

$$(4.7) \quad R^n: X^o \cup Y^o \cup s \rightarrow \mathbf{H}^+ \cup \mathbf{H}^- \cup R^n(s)$$

is conformal. So neighbors are conformal reflections of each other along shared sides. For each n , the cylinders of order n form a tiling of the sphere. One can construct the tiling from one cylinder, since the other cylinders of given order can be constructed by repeated reflection.

A union of cylinders $\mathbf{X} = \bigcup_{j \in J} X_j$ of order n may be viewed as a two-dimensional simplicial complex $\Sigma(\mathbf{X})$, where n -cylinders, n -sides, and n -corners are the faces, edges, and vertices. The *combinatorial type* of \mathbf{X} is $\Sigma(\mathbf{X})$ together with the type of each n -cylinder, n -side, and n -corner in \mathbf{X} . Note that here we do not require any information about cylinders of order $k \neq n$ that may be contained in \mathbf{X} . Two unions of cylinders

$$(4.8) \quad \begin{aligned} \mathbf{X} &= \bigcup_{j \in J} X_j, \quad |X_j| = n \text{ and} \\ \mathbf{Y} &= \bigcup_{i \in I} Y_i, \quad |Y_i| = m \end{aligned}$$

are called *combinatorially equivalent* if they are of the same combinatorial type. More precisely if there is a (simplicial complex) isomorphism

$$(4.9) \quad \Phi: \Sigma(\mathbf{X}) \rightarrow \Sigma(\mathbf{Y}),$$

such that for each n -cylinder X , n -side s , and n -corner c in \mathbf{X} the types of X and $\Phi(X)$, s and $\Phi(s)$, c and $\Phi(c)$ are all the same. Combinatorial equivalence implies conformal equivalence.

Lemma 4.3. *Let \mathbf{X} and \mathbf{Y} as in (4.8) be combinatorially equivalent. Then there is a conformal map*

$$g: \mathbf{X}^o \rightarrow \mathbf{Y}^o.$$

Furthermore $n + k$ -(cylinders, sides, corners) in \mathbf{X}^o are mapped to $m + k$ -(cylinders, sides, corners) in \mathbf{Y}^o by g (for any $k \geq 0$).

Proof. Let Φ be as in (4.9). Pick an n -cylinder $X_1 \subset \mathbf{X}$. Let $X_2 \subset \mathbf{X}$ be a neighbor of X_1 with common side s_1 . Let $Y_1 := \Phi(X_1)$, $Y_2 := \Phi(X_2)$, and $t_1 := \Phi(s_1)$. By equation (4.7) the functions

$$\begin{aligned} R^n: X_1^o \cup X_2^o \cup s_1 &\rightarrow \mathbf{H}^+ \cup \mathbf{H}^- \cup \text{type of } s_1, \\ R^m: Y_1^o \cup Y_2^o \cup t_1 &\rightarrow \mathbf{H}^+ \cup \mathbf{H}^- \cup \text{type of } t_1 \end{aligned}$$

are conformal. The first function maps $n + k$ -(cylinders, sides, corners) to k -(cylinders, sides, corners), the second function maps $m + k$ -(cylinders, sides, corners) to k -(cylinders, sides, corners). Since s_1 and t_1 are of the same type this gives us a function

$$g: X_1^o \cup X_2^o \cup s_1 \rightarrow Y_1^o \cup Y_2^o \cup t_1$$

which is conformal and maps (cylinders, sides, and corners) in the desired fashion. We can now proceed to further neighbors to extend g to the whole component of \mathbf{X} which contains X_1^o (corners lying inside are of course removable singularities). On the other components g is constructed in the same way. \square

The proof of Theorem 4.2 follows essentially from the next two lemmas.

Lemma 4.4. *There is a constant $C > 0$, such that for all n -cylinders X and Y for which $X \cap Y = \emptyset$, we have*

$$C \operatorname{dist}(X, Y) \geq \operatorname{diam} X.$$

Proof. Let X and Y be as above. Let

$$(4.10) \quad \mathbf{X} := \bigcup_{|X'|=|X|, X' \cap X \neq \emptyset} X'.$$

Each cylinder X' in the above union shares at least a corner c with X . Since at c , $2 \operatorname{deg}_{R|X|}(c)$ cylinders intersect, there are by (4.6) only finitely many cylinders in the union (4.10). For each cylinder X' , there are only finitely many possibilities for the types of its sides and corners. So there are only finitely many different combinatorial types of unions \mathbf{X} as above. For the modulus of the annulus $A := \mathbf{X}^o \setminus X$ we therefore have

$$(4.11) \quad M(A) \geq \operatorname{const} > 0,$$

since the modulus for each combinatorial type is the same by Lemma 4.3.

Remark. It might happen that A is not an annulus (that $\widehat{\mathbf{C}} \setminus A$ has more than two components). Still A contains an annulus A' that separates X from Y with a modulus bounded below.

Let $\operatorname{comp}(Y)$ be the component of $\widehat{\mathbf{C}} \setminus A$ that contains Y . It is well known that the modulus behaves as

$$M(A) \sim \frac{\operatorname{dist}(X, \operatorname{comp}(Y))}{\min\{\operatorname{diam}(X), \operatorname{diam}(\operatorname{comp}(Y))\}}$$

(meaning that both sides simultaneously go to 0 and ∞). If the order n is sufficiently large we have $\operatorname{diam}(X) \leq \operatorname{diam}(\operatorname{comp}(Y))$.

This finishes the proof, since A separates X and Y . \square

Lemma 4.5. *Let X, Y be n -cylinders such that $X \cap Y \neq \emptyset$. Then*

$$\operatorname{diam} X \asymp \operatorname{diam} Y.$$

Proof. Let X and Y be as above. Then X and Y must intersect at least in a corner. By (4.6) it is enough to assume that X and Y are neighbors. Consider

$$\mathbf{Z} := \bigcup_{Z \cap (X \cup Y) \neq \emptyset, |Z|=n} Z.$$

There are only finitely many different combinatorial types of such \mathbf{Z} . The set $X \cup Y$ is compactly contained in \mathbf{Z}^o . The statement now follows from Koebe distortion theorem and Lemma 4.3. \square

Proof of Theorem 4.2. One can easily check that T is doubling. To do this first check that T is doubling in the combinatorial pseudometric δ . Any cylinder of δ -diameter 3^{-n} can be covered by 13 cylinders of δ -diameter 3^{-n-1} . Any ball of δ -diameter 3^{-n} is a union of at most 10 cylinders of δ -diameter 3^{-n} . It follows from Lemma 2.2 and (3.1) that T is doubling.

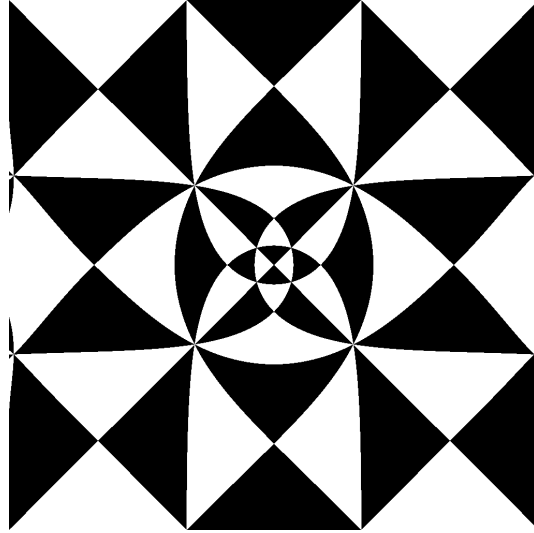


Figure 6. Embedding of cylinders of second order.

Since T is also connected it is enough to show that f is weakly quasymmetric, by Theorem 2.1. To avoid switching back and forth between points in T and $\overline{\mathbf{H}}^+$ we regard δ as a function on $\widehat{\mathbf{C}} \times \widehat{\mathbf{C}}$:

$$\delta(x, y) := 3^{-n},$$

where n is the smallest number such that there are disjoint n -cylinders $X \ni x$, $Y \ni y$ in $\widehat{\mathbf{C}}$. We need to show that there is a $C > 0$ such that

$$\delta(x, y) \leq \delta(x, z) \Rightarrow |x - y| \leq C|x - z|,$$

for all $x, y \in \widehat{\mathbf{C}}$. All cylinders and points are now considered to be living in $\widehat{\mathbf{C}}$.

Suppose $\delta(x, y) \leq \delta(x, z)$, $\delta(x, y) = 3^{-n}$, so for $X_{n-1} \ni x$, $Y_{n-1} \ni y$, $|X_{n-1}| = |Y_{n-1}| = n - 1$, we have $X_{n-1} \cap Y_{n-1} \neq \emptyset$. By Lemma 4.5

$$|x - y| \leq \text{diam } X_{n-1} + \text{diam } Y_{n-1} \leq C \text{diam } X_{n-1} \leq C' \text{diam } X_n,$$

for any $X_n \ni x$, $|X_n| = n$, since X_{n-1} contains only finitely many cylinders of order n which have comparable diameter by Lemma 4.5.

Since $\delta(x, z) \geq 3^{-n}$, there are disjoint n -cylinders $X_n \ni x$, $Z_n \ni z$. So by Lemma 4.4

$$|x - y| \leq C' \text{diam } X_n \leq C'' \text{dist}(X_n, Z_n) \leq C''|x - z|,$$

which proves the theorem. \square

Figures 6 and 7 show the embedding. They show the part of \mathbf{H}^+ that corresponds to the square (a_2, c_2, a_3, c_3) in Figure 5.

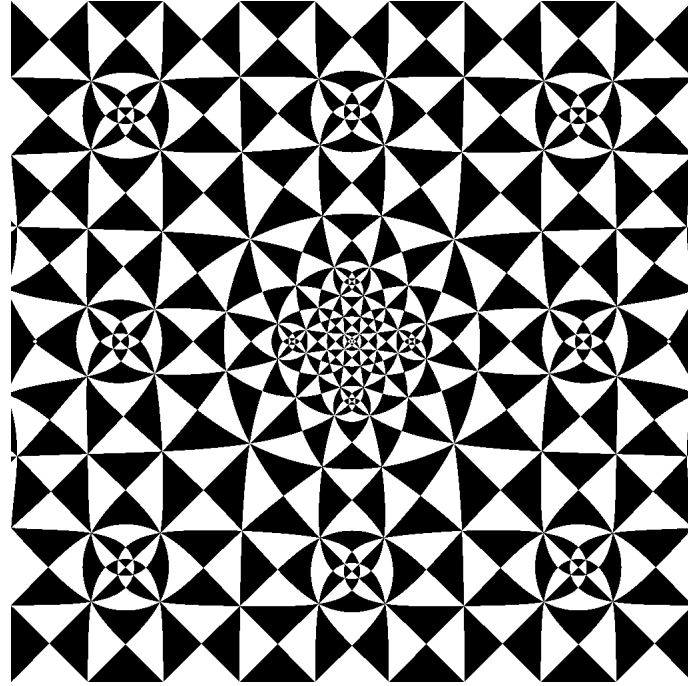


Figure 7. Embedding of cylinders of third order.

5. General form of the theorem

Let R be a rational map satisfying the following conditions:

- $R(z) = \overline{R(\bar{z})}$;
- for the postcritical set $P_R := \{R^n(c) : c \text{ critical point of } R, n \geq 1\}$ we require: P_R is finite, $P_R \subset \widehat{\mathbf{R}}$, and every periodic cycle in P_R is repelling.

The second condition implies that R is subhyperbolic. Such a map divides the sphere in a natural way into cylinders of order n : the preimages of $\overline{\mathbf{H}^+}$ and $\overline{\mathbf{H}^-}$ under R^n . As before these induce a combinatorial pseudometric:

$$\delta(x, y) := \varrho^n,$$

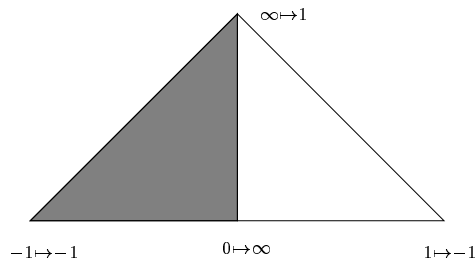
where $\varrho \in (0, 1)$, and n is the smallest number such that $X_n \cap Y_n = \emptyset$, for all cylinders $X_n \ni x, Y_n \ni y$ of order n . We have

Theorem 5.1. *Let R and δ be as above, then*

$$\text{id}: (\widehat{\mathbf{C}}, \delta) \rightarrow (\widehat{\mathbf{C}}, \text{spherical metric})$$

is quasymmetric.

The proof is the same as the proof of Theorem 4.2 and will not be repeated.

Figure 8. R_1 .

6. Origami with rational maps

In this section we give further examples of rational maps which represent a subdivision rule. In the case that such a subdivision rule describes a surface whose metric is quasisymmetrically comparable to the combinatorial pseudometric, Theorem 5.1 gives a quasisymmetric embedding. The construction is always the same as in Section 3: a generator consisting of triangles (in one case squares) symmetric on common sides is mapped to $\overline{\mathbf{H}}^+$ by a Riemann map, which is normalized by requiring that corners labeled by “ $a \mapsto b$ ” get mapped to a . The rational function is defined by mapping each of the “white” image triangles (or squares) to $\overline{\mathbf{H}}^+$ and each of the “black” ones to $\overline{\mathbf{H}}^-$ by a Riemann map, which is normalized by requiring that corners labeled by “ $\mapsto b$ ” get mapped to b . As before the reflection principle ensures that the map is holomorphic in $\overline{\mathbf{H}}^+$, and by $R(z) = \overline{R(\bar{z})}$ we define R on the whole sphere, so R is a rational map.

The generator together with the data on how corners are to be mapped defines the map and so may be viewed as an alternative description of the map. In fact important properties such as critical points and poles, and their order can be immediately read off. Similarly to (3.3) and (3.4), we can express the rational maps in terms of the critical points and poles. Again one gets a system of equations for the critical points and poles. In the easier cases this can be solved by elementary means. In the more difficult cases we used Don Marshall’s zipper as well as the Schwarz–Christoffel toolbox

(<http://www.math.udel.edu/~driscoll/SC/>)

by Tobin Driscoll and Nick Trefethen to get numerical values for the critical points. With a Newton method the precision can be increased arbitrarily. Often the coefficients of the rational maps turn out to be rational numbers. From this one often can guess the precise values of the critical points. One can confirm these guesses by showing that they satisfy the system of equations exactly; we used Mathematica for this.

Another nice way to visualize these maps is to actually cut the generator out of paper. The generators should be viewed as a sphere, the two sides representing

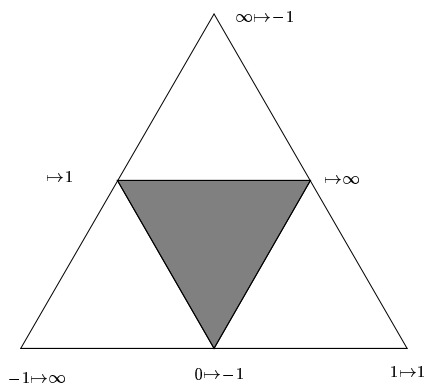


Figure 9. R_2 .

\mathbf{H}^+ and \mathbf{H}^- . One can then fold the generator such that white triangles land on the front, black ones on the back, resulting in a small triangle. This is again viewed as the sphere, the white side being interpreted as \mathbf{H}^+ , the black side as \mathbf{H}^- , thereby illustrating the covering behavior of the rational map.

Hopefully this explains our use of the word “origami”.

6.1. Euclidean subdivisions. The first four examples have the property that their generator is similar to its pieces. Thus, when one cuts the generator out of paper and folds as suggested above, the resulting piece can be folded again. This represents the second iterate, another folding the third iterate, and so on.

The functions given by Figures 8, 9, 10, and 11 are

$$\begin{aligned}
 R_1 &= 1 - \frac{2}{z^2}, \\
 R_2 &= 1 - 2 \frac{(z-1)(z+3)^3}{(z+1)(z-3)^3}, \\
 R_3 &= 1 + 8 \frac{z(z^2-1)}{(z^2-2z-1)^2}, \\
 R_4 &= 1 - \frac{(3z+1)^3}{(9z-1)^2}.
 \end{aligned}$$

The function R_3 is the only example considered here where the generator consists of squares, however the Riemann maps from which R_3 is constructed are well-defined. Indeed, let Q be a square with vertices v_1, v_2, v_3, v_4 and $f: Q \rightarrow \mathbf{H}^+$ be a Riemann map normalized by $f(v_1) = -1$, $f(v_2) = 0$ and $f(v_3) = 1$. Then we have by symmetry $f(v_4) = \infty$.

To further illustrate these examples we need the notion of *orbifolds*, see [McM] and [Mil] for definitions and properties. The signature or ramification index of the orbifold of R_1 is $(2, 4, 4)$, of R_2 is $(3, 3, 3)$, of R_3 is $(2, 2, 2, 2)$, and of R_4 is

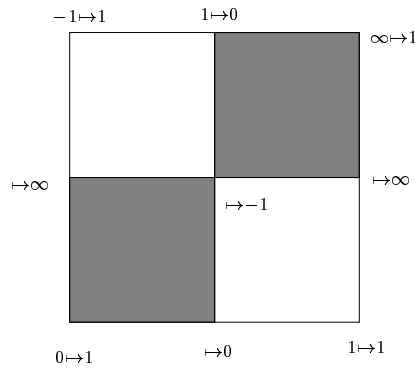


Figure 10. R_3 .

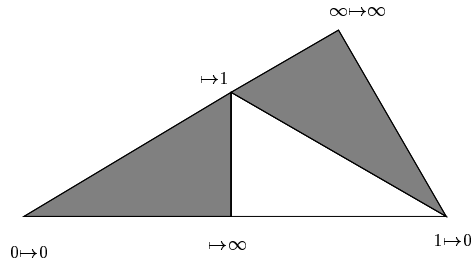


Figure 11. R_4 .

(2, 3, 6). All these orbifolds are *euclidean*, meaning that their universal orbifold covering maps have domain \mathbf{C} . In fact the above signatures are the only ones that can occur for euclidean orbifolds over $\widehat{\mathbf{C}}$, see [McM]. The mapping behavior of the universal orbifold covering maps f_j is indicated in Figure 12 (again white triangles map to \mathbf{H}^+ , and black ones to \mathbf{H}^-), they are elliptic functions. We have

$$\begin{aligned} f_1(\sqrt{2} e^{3\pi i/4} z) &= R_1(f_1(z)), \\ f_2(2z) &= R_2(f_2(z)), \\ f_3(2iz) &= R_3(f_3(z)), \\ f_4(\sqrt{3} e^{\pi i/6} z) &= R_4(f_4(z)). \end{aligned}$$

So $R_1, R_2, R_3,$ and R_4 are all Lattès type functions.

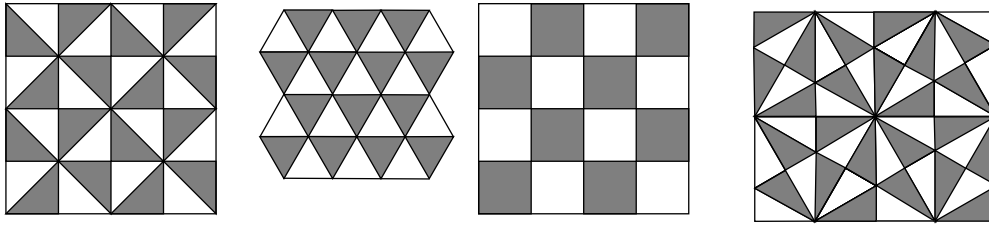


Figure 12. Universal orbifold coverings for R_1 , R_2 , R_3 , and R_4 .

6.2. The barycentric subdivision rule. Figure 13 shows the barycentric subdivision rule which is generated by

$$R_5 = 1 - \frac{54(z^2 - 1)^2}{(z^2 + 3)^3}.$$

This map was already found in [CFKP]. It is an example where Cannon’s combinatorial Riemann mapping theorem cannot be used. Of course our Theorem 5.1 does not work as well, since all critical values are again critical points and hence all cycles in P_R are superattracting. In fact one can show that the diameter of the cylinders generated by this function fail to go to zero with their order.

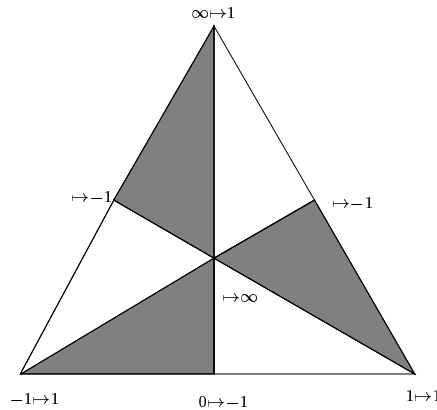


Figure 13. R_5 .

6.3. Variants of the snowball. The next three examples embed variants of the snowball.

We start with an equilateral triangle which is divided into 4 equilateral triangles as in Figure 9. On the middle triangle put a tetrahedron, which produces the generator of a self similar surface consisting of 6 equilateral triangles. Cut the surface into 6 pieces along the symmetry axes. We restrict our attention to one such piece T_6 (see Figure 14). Simultaneously cut each triangle into 6 as in the barycentric subdivision in Figure 13. T_6 consists of 6 scaled (and possibly reflected) copies of itself. The generator of T_6 consists of 6 triangles. One can

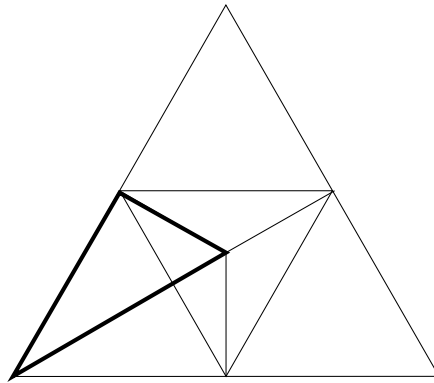


Figure 14. Generator of the tetrahedron-snowball.

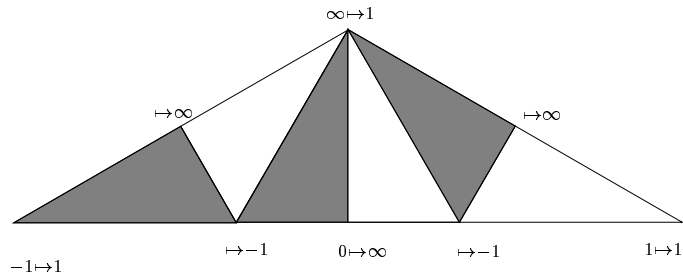


Figure 15. R_6 .

construct T_6 by replacing in each step each of these triangles by a scaled (and possibly reflected) copy of the generator. The generator of T_6 can be folded flat in the plane (see Figure 15). The corresponding function is given by

$$R_6 = 2 \left(\frac{3}{4} \right)^3 \frac{z^2 - 1}{z^2 \left(z^2 - \frac{9}{8} \right)^2} + 1.$$

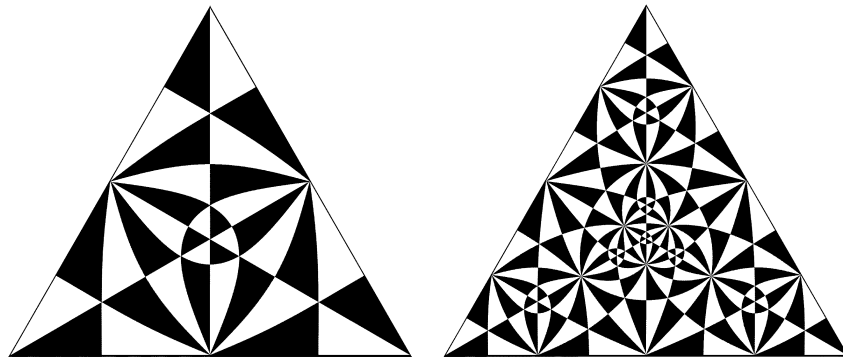


Figure 16. Embedding of cylinders of first and second order by R_6 .

Figure 16 shows how R_6 embeds cylinders of first and second order.

Another selfsimilar surface is obtained when one puts an octahedron instead of a tetrahedron on the middle triangle. The rest of the construction is analogous to the last. Again the surface is cut into 6 pieces. Figure 17 shows the generator and how the corresponding rational map is constructed. Again the construction embeds the surface quasisymmetrically. The thick lines are lines along which the generator was folded when it was mapped into the plane. We have

$$R_7 = \frac{z(z-1)^5(z+80)^4}{1000\left(z^3 - \frac{213}{8}z^2 - 132z - \frac{32}{5}\right)^3}.$$

A third example of this type is obtained by putting an icosahedron on the middle triangle. Again the generator and every face is subdivided into 6 pieces. As before the generator can be folded into the plane. See Figure 18 for the generator and the corresponding construction of the rational map. The thick lines are the ones along which the generator has been folded. We obtain

$$R_8 = \frac{\lambda z(z-1)^6(z^3 + a_2z^2 + a_1z + a_0)^5}{(z^7 + b_6z^6 + b_5z^5 + b_4z^4 + b_3z^3 + b_2z^2 + b_1z + b_0)^3},$$

where

$$\begin{aligned} \lambda &= \frac{2}{5^2 \cdot 11^2}, \\ a_2 &= \frac{3 \cdot 17 \cdot 1439}{2^4 \cdot 5}, \\ a_1 &= -\frac{3 \cdot 5^4 \cdot 11 \cdot 17}{2^3}, \\ a_0 &= -\frac{5^9 \cdot 11}{2^4}, \\ b_6 &= -\frac{378223}{2^7 \cdot 5}, \\ b_5 &= -\frac{3 \cdot 863 \cdot 24907}{2^6 \cdot 5^2}, \\ b_4 &= -\frac{601 \cdot 1381 \cdot 689761}{2^7 \cdot 5^4}, \\ b_3 &= \frac{5 \cdot 19 \cdot 103 \cdot 113 \cdot 1399}{2^5}, \\ b_2 &= -\frac{3 \cdot 5^6 \cdot 19 \cdot 53 \cdot 3001}{2^7}, \\ b_1 &= -\frac{5^{11} \cdot 3907}{2^6}, \\ b_0 &= -\frac{5^{16}}{2^7 \cdot 11}. \end{aligned}$$

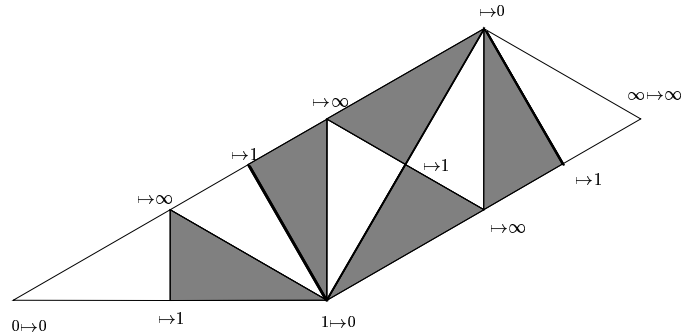


Figure 17. R_7 .

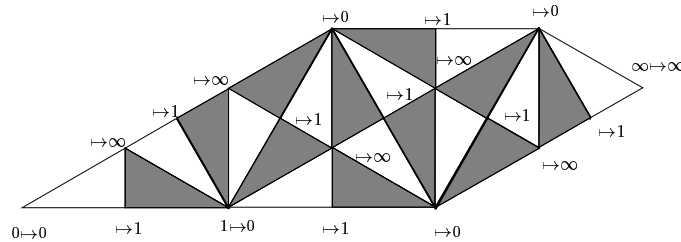


Figure 18. R_8 .

While there is extremely strong numerical evidence that these are indeed the precise values, it turns out to be too difficult to rigorously check that. So the above values are to be understood as the conjectured precise values.

As for the snowball, it is easy to check that for the three previous examples the internal metric is comparable to the combinatorial pseudometric. Since all the conditions for Theorem 5.1 are satisfied this produces a quasisymmetric embedding.

6.4. The Xmas tree. The three preceding examples have the disadvantage that as surfaces in \mathbf{R}^3 they have self-intersections. The next class of examples are surfaces embedded in \mathbf{R}^3 (without self-intersections) whose Hausdorff dimension can be arbitrarily close to 3. The construction is similar to the snowball, again we have a generator built from small squares. In each iterative step each square gets replaced by a scaled copy of the generator.

The generator of the n -Xmas tree is given the following way. Start with a unit square. Divide the square into $(4n+5)^2$ squares of sidelength $s = 1/(4n+5)$. On the middle square put a cube of sidelength s (an s -cube). On this put a layer of $(4(n-1)+3)^2$ s -cubes, arranged in a square of sidelength $s(4(n-1)+3)$.

On top of this layer put an s -cube in the middle. On this put another layer

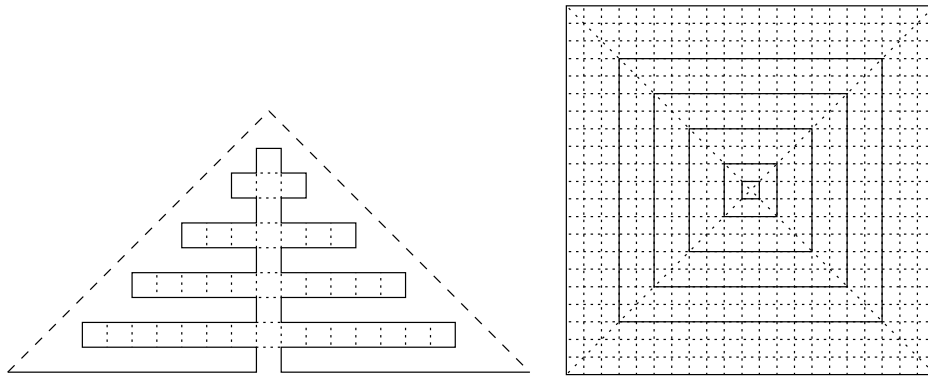


Figure 19. Generator of the 4-Xmas tree from the side and the top.

of $(4(n - 2) + 3)^2$ s -cubes, arranged in a square of sidelength $s(4(n - 2) + 3)$, and so on. Figure 19 shows the generator of the 4-Xmas tree from the side and from above.

A short calculation shows that the generator of the n -Xmas tree is made from $\#(\text{squares}) = \frac{1}{3}(32n^3 + 96n^2 + 136n + 12)$ squares of sidelength $s = 1/(4n + 5)$ (the exact number is not important, only that $\#(\text{squares}) = O(n^3)$). We have the following facts.

- The generator can be placed inside a rectangular pyramid which is indicated in Figure 19. This ensures that the resulting surface is embedded in \mathbf{R}^3 without self-intersections.
- This also implies that the Xmas tree satisfies the *open set condition*, so the Hausdorff dimension is (see [F, p. 118, Theorem 9.3])

$$\frac{\log \#(\text{squares})}{\log(4n + 5)} \rightarrow 3, \quad \text{as } n \rightarrow \infty.$$

To embed the Xmas tree quasisymmetrically on the plane (or rather on the sphere), use the same procedure as before: cut the generator into 4 pieces along the diagonals. Again consider only one such piece G . Simultaneously each square gets divided into 4 triangles. As before G can be folded in the plane, see Figure 20. From this we construct the rational map R_X that mirrors the selfsimilarity. It is not hard to check that on the Xmas tree the induced metric from \mathbf{R}^3 is comparable to the internal metric, which is comparable to the combinatorial pseudometric. Theorem 5.1 again shows that R_X embeds our surface quasisymmetrically.

6.5. The n -gon subdivision rule. In [BS] the pentagonal subdivision rule is studied. It consists of replacing each pentagon in each step by 6 pentagons as in Figure 21. In [CFKP] it was shown that this subdivision can be represented by the rational map

$$(6.1) \quad R_{5\text{-gon}} = \frac{2z(z + \frac{9}{16})^5}{27(z - \frac{3}{128})^3(z - 1)^2}.$$

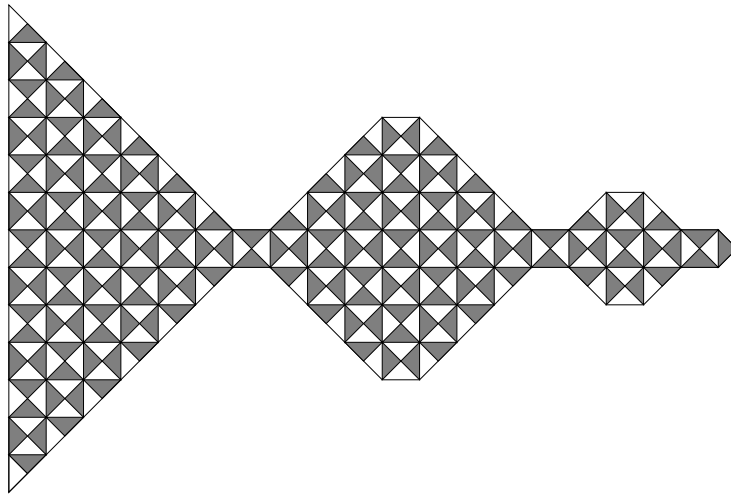
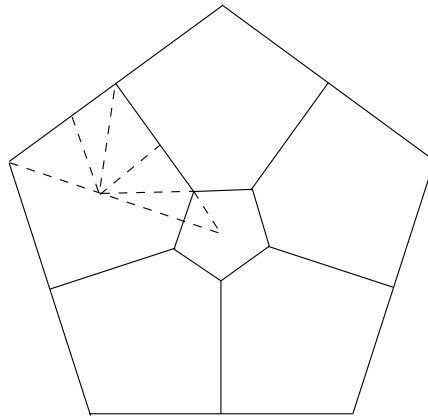
Figure 20. G for the 2-Xmas tree folded in the plane.

Figure 21. The pentagonal subdivision rule.

To do this, Figure 21 is cut along the diagonals into 10 pieces. Only one such piece is considered as a generator. Simultaneously the 6 pentagons are cut into 10 pieces as well.

The map in (6.1) may be explicitly constructed using the method of this section. The generator can be realized by triangles symmetric on common edges, as in Figure 22, which constructs the map. $R_{5\text{-gon}}$ equips the subdivision with a conformal structure (see [C] and [CFP] for this). This may be seen by using Theorem 5.1.

An analogous construction can actually be done for any n -gon, where $n \geq 5$ and odd. See Figure 23 for the 7-gon. The rational map in this case is

$$R_{7\text{-gon}} = \lambda \frac{(z-1)z^2(z-b_1)^2(z-b_2)^3}{(z-c)^7} + 1,$$

where $\lambda = -0.00461795\dots$, $b_1 = -27.9055\dots$, $b_2 = 0.856734\dots$, $c = 1.60219\dots$. Again by Theorem 5.1 this map equips the subdivision with a conformal structure.

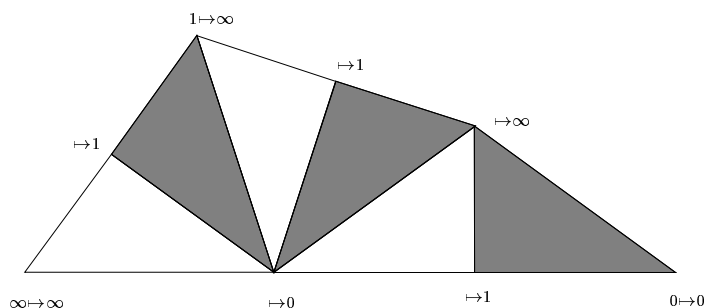


Figure 22. Construction of $R_{5\text{-gon}}$.

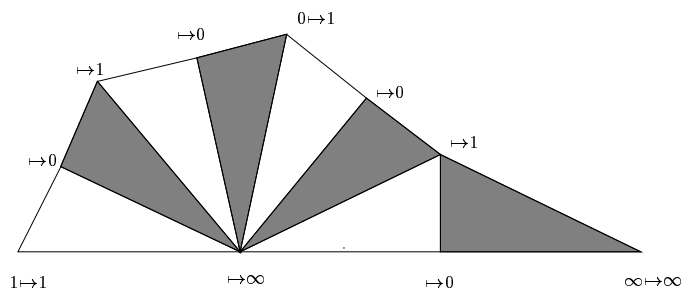


Figure 23. Construction of $R_{7\text{-gon}}$.

For n even and $n \geq 4$ an analogous subdivision can be defined as well (see Figure 24). The corresponding rational map is

$$R_{4\text{-gon}} = 1 - \frac{(z - 1)^2(z + 9)^3}{25\left(z^2 + \frac{27}{5}\right)^2}.$$

However, for n even the maps $R_{n\text{-gon}}$ have critical values that are themselves critical points.

References

- [BK] BONK, M., and B. KLEINER: Quasisymmetric parametrizations of two-dimensional metric spheres. - Invent. Math. (to appear).
- [BS] BOWERS, P.L., and K. STEPHENSON: A “regular” pentagonal tiling of the plane. - Conform. Geom. Dyn. 1, 1997, 58–86 (electronic).
- [C] CANNON, J.W.: The combinatorial Riemann mapping theorem. - Acta Math. 173, 1994, 155–234.
- [CFP] CANNON, J.W., W.J. FLOYD, and R. PARRY: Finite subdivision rules. - Preprint on <http://www.math.vt.edu/people/index.html>.

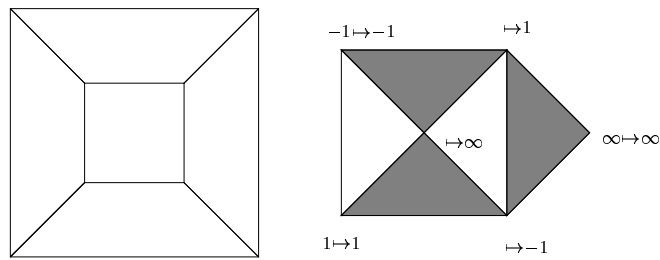


Figure 24. Tetragon subdivision rule and generator.

- [CFKP] CANNON, J.W., W.J. FLOYD, R. KENYON, and R. PARRY: Constructing rational maps from subdivision rules. - To appear.
- [CG] CARLESON, L., and T.H. GAMELIN: Complex Dynamics. - Springer-Verlag, 1993.
- [H] HEINONEN, J.: Lectures on Analysis on Metric Spaces. - Universitext, Springer-Verlag, New York, 2001.
- [F] FALCONER, K.: Fractal Geometry. Mathematical Foundations and Applications. - Wiley, Chichester, 1990.
- [Mil] MILNOR, J.: Dynamics in One Complex Variable. Introductory Lectures. - Vieweg & Sohn, Braunschweig, 1999. (Also available as preprint under <http://www.math.sunysb.edu/cgi-bin/preprint.pl/~ims90-5>)
- [McM] MCMULLEN, C.T.: Complex Dynamics and Renormalization. - Ann. of Math. Stud. 135, Princeton Univ. Press, Princeton, NJ, 1994.
- [TV] TUKIA, P., and J. VÄISÄLÄ: Quasisymmetric embeddings of metric spaces. - Ann. Acad. Sci. Fenn. Ser. A I Math. 5, 1980, 97–114.

Received 17 December 2001